Eur. Phys. J. B **30**, 211–218 (2002)
DOI: 10.1140/epjb/e2002-00376-5

THE EUROPEAN PHYSICAL JOURNAL B

Control of electron transfer in disordered DNA under the impact of viscous damping and an external periodic field

D. Hennig[a]

Freie Universität Berlin, Fachbereich Physik, Institut für Theoretische Physik, Arnimallee 14, 14195 Berlin, Germany

Received 5 July 2002
Published online 29 November 2002 –

Abstract. We investigate the influence of energetic disorder, viscous damping and an external field on the electron transfer (ET) in DNA. The double helix structure of the λ-form of DNA is modeled by a steric oscillator network. In the context of the base-pair picture two different kinds of modes representing twist motions of the base pairs and H-bond distortions are coupled to the electron amplitude. Through the nonlinear interaction between the electronic and the vibrational degrees of freedom localized stationary states in the form of standing electron-vibron breathers are produced which we derive with a stationary map method. We show that in the presence of additional energetic disorder the degree of localization of such breathers is enhanced. It is demonstrated how an applied electric field initiates the long-range coherent motion of breathers along the bases of a DNA strand. These moving electron-vibron breathers, absorbing energy from the applied field, sustain energetic losses due to the viscous friction caused by the aqueous solvent as well as the impact of a moderate amount of energetic disorder. Moreover, it is illustrated that with the choice of the amplitude and frequency of the external field, the breather can be steered to a desired lattice position achieving control of the ET.

PACS. 87.15.-v Biomolecules: structure and physical properties – 63.20.Kr Phonon-electron and phonon-phonon interactions – 63.20.Ry Anharmonic lattice modes

1 Introduction

Electronic transport (ET) through DNA has recently attracted a lot of attention, especially in the context of its role for biological functions such as the repair mechanism after radiation damage and biosynthesis [1]. It was proposed that ET through DNA proceeds along a one-dimensional pathway constituted by the overlap between π-orbitals in neighboring base pairs [2]. Recent measurements have indeed suggested that DNA forms an effective one-dimensional molecular wire [3–11] which offers promising applications in molecular electronics based on biomaterials [12,13]. In contrast, it has also been reported that DNA is insulting [14] so that the findings concerning conductivity through DNA remain controversial.

There have been different attempts to model theoretically the charge transport in DNA utilizing transport *via* coherent tunneling [2], incoherent phonon-assisted hopping [15,16], classical diffusion under the conditions of thermal fluctuations [17], variable range hopping between localized states [18] and charge carriers assisted by solitons [19] and polarons [20–22]. In fact in a recent paper it has been argued that the polaron picture is relevant for the hole transport in DNA [23].

In the current study we propose a possible control mechanism of ET in DNA relying on the impact of an applied external field. For the modeling of the transfer mechanism we use a nonlinear approach based on the concept of polarons and breather solutions. The structure of the bent double helix of λ-DNA is modeled by a steric network of oscillators in the frame of the base pair picture [24–26] taking into account deformations of the hydrogen bond within a base pair and twist motions between adjacent base pairs. The electron motion is described by a tight-binding system. The nonlinear interaction between the electron and the vibrational modes cause the formation of polarons and (standing) electron-vibron breathers. We pay special attention to the influence of an external field with respect to the realizable control of the ET under the condition of energy dissipation due to the influence of the viscous solvent and with the additional inclusion of energetic disorder. The external field control of rate processes and biochemical reactions has become of considerable interest recently [27–31].

The paper is organized as follows: In the first section we describe the model for the ET along the bent structure of the double helix of λ-DNA in the presence of an external field and with viscous friction. In the second section we discuss briefly the features of the static electron-vibron breather solutions of the nonlinear lattice system with and

[a] e-mail: hennigd@physik.fu-berlin.de

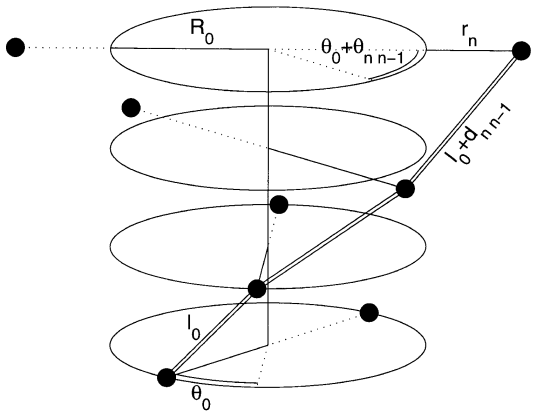

Fig. 1. Schematic representation of the helicoidal structure of the DNA model.

without energetic disorder. Subsequently, in the third section we consider the activation of electron-vibron breather motion and the control of ET through the external field. Finally, we summarize and discuss the results.

2 Model for damped and driven ET in DNA

In our DNA model we cover the basic features of the DNA double helix structure and consider the latter as a bent double-stranded system for which in the frame of a base pair picture the bases are treated as single nondeformable entities. The helicoidal structure of DNA is then conveniently described in a cylindrical reference system where each base pair possesses two degrees of freedom, namely a radial variable measuring the transversal displacements of the base pair (that is, deformations of the H-bond) and the angle with a reference axis in a plane perpendicular to the helix backbone which defines the twist of the helix [26]. In Figure 1 we represent a sketch of the structure of the DNA model.

The charge migration process is influenced by the dominant vibrational modes of DNA stemming from transverse vibrations of the bases relative to each other, *viz.*, the stretchings/compressions of the base pair distance within a base pair plane and the torsional variations of the helicoidal twist [17–32]. The influence of other vibrational degrees of freedom (*e.g.*, longitudinal acoustic phonons along the strands are significantly restrained by the backbone) can be discarded and the motion is restricted to the base pair planes [33].

The Hamiltonian for the ET along a strand in DNA under the influence of an external electric field consists of four parts

$$H = H_{el} + H_{rad} + H_{twist} + H_{field}\,, \tag{1}$$

where H_{el} is the part which describes the ET across the base pairs, H_{rad} and H_{twist} represent the H-bond vibrations and the relative twist angle between two consecutive base pairs, respectively. The last term H_{field} represents the Hamiltonian of the external field. The electronic part is given by a tight-binding model

$$H_{el} = \sum_n E_n\,|c_n|^2 - V_{n\,n-1}\,\left(c_n^* c_{n-1} + c_n c_{n-1}^*\right)\,, \tag{2}$$

with the index n denoting the site of the nth base pair and c_n determines the probability that the electron occupies this site. E_n is the local electronic energy and V_{nn-1} is the transfer matrix element which is responsible for the transport of the electron across the stacked base pairs. We make the usual assumption that ET takes place solely along the base pair sequence on a strand excluding ET across base pairs (see, *e.g.*, Ref. [2]).

The radial vibronic part H_{rad} models dynamical deviations from the equilibrium length of the hydrogen bonds linking a base pair. With a classical and harmonic treatment H_{rad} is given by

$$H_{rad} = \frac{1}{2}\sum_n M_n\,\left[\,\dot{r}_n^{\,2} \,+\, \Omega_r^2\, r_n^2\,\right]\,. \tag{3}$$

The radial coordinates r_n quantify the radial displacements of the base units from their equilibrium positions along the line bridging two bases of a base pair within the base pair plane. We remark that polaronic ET is connected only with small structural deformations of the hydrogen bonds so that the harmonic approximation of the bond vibrations is in order [17]. M denotes the reduced mass and Ω_r is the harmonic frequency of the bond vibration.

The Hamiltonian for the twist motion is given by

$$H_{twist} = \frac{1}{2}\sum_n J_n\,\left[\,\dot{\theta}^2_{n\,n-1} \,+\, \Omega_\theta^2\,\theta^2_{n\,n-1}\right]\,, \tag{4}$$

where $\theta_{n\,n-1}$ is the relative angle between two adjacent base pairs measuring the displacement from the equilibrium twist angle θ_0, J_n is the reduced moment of inertia and Ω_θ is the frequency of the twist vibrations. The dynamics of the angular twist and radial vibrational motions evolve independently on distinct time scales and can be regarded as decoupled degrees of freedom in the harmonic approximation of the lattice dynamics of a DNA oscillator network (see also [34]).

The interaction between the electronic variable c_n and the structure variables r_n and $\theta_{n\,n-1}$ originates from the parameter dependence of the electronic parameters E_n and $V_{n\,n-1}$. The diagonal term expressing the most efficient coupling is of the form

$$E_n = E_n^0 + k\,r_n\,, \tag{5}$$

and reflects the modulation of the on-site electronic energy E_n^0 by the radial vibrations of the base pairs [17–22]. In turn the actual charge occupation has its impact on the local radial distortion of the helix. We include also static diagonal disorder in the on-site electronic energy E_n^0. The random energy values are simulated by random potentials $E_n^0 - \bar{E} \in [-\Delta E, \Delta E]$ with mean value $\bar{E}$ and widths ΔE. As the transfer matrix elements $V_{n\,n-1}$

are concerned we assume that they depend on the three-dimensional distance between two consecutive bases in the following fashion

$$V_{n\,n-1} = V_0\,(1 - \alpha\, d_{n\,n-1})\,. \tag{6}$$

The quantity α regulates how strong $V_{n\,n-1}$ is influenced by the distance and the latter is determined by

$$d_{n\,n-1} = \big\{a^2 + (R_0 + r_n)^2 + (R_0 + r_{n-1})^2 - 2(R_0 + r_n)(R_0 + r_{n-1})\,\cos(\theta_0 + \theta_{n\,n-1})\big\}^{1/2} - l_0\,, \tag{7}$$

with

$$l_0 = \sqrt{a^2 + 4R_0^2\,\sin^2(\theta_0/2)}\,, \tag{8}$$

and a is the distance between two neighboring base pair planes measured in z-direction. Expanding the expression (7) up to first order around the equilibrium positions yields

$$d_{n\,n-1} \simeq \frac{R_0}{l_0}\,\left[\,(\,1 - \cos\theta_0\,)\,(r_n + r_{n-1}) \,+\, \sin\theta_0\, R_0\, \theta_{n\,n-1}\,\right]\,. \tag{9}$$

The effect of an external electric field on the ET in DNA is described by the Hamiltonian representing the electron-field interaction

$$H_{field} = -e\,E(t) \sum_n n\,a\,|c_n|^2\,, \tag{10}$$

with $E(t) = E_0 \sin(\omega t)$ is the time-dependent periodic electric field directed along the strands and e is the electron charge.

Realistic parameters for DNA molecules are given by [26–32]: $a = 3.4$ Å, $R_0 \approx 10$ Å, $\theta_0 = 36°$, $J = 4.982\times10^{-45}\,\mathrm{kg\,m^2}$, $\Omega_\theta = [0.526-0.744]\times10^{12}\,\mathrm{s^{-1}}$, $\Omega_r = 6.252\times10^{12}\,\mathrm{s^{-1}}$, $V_0 \simeq 0.1$ eV and $M = 4.982\times10^{-25}$ kg.

With a time scaling $t \to \Omega_r\, t$ it is appropriate to introduce the dimensionless quantities:

$$\tilde r_n = \sqrt{\frac{M\Omega_r^2}{V_0}}\,r_n\,, \qquad \tilde k_n = \frac{k_n}{\sqrt{M\Omega_r^2 V_0}}\,, \qquad \tilde E_n^0 = \frac{E_n^0}{V_0} \tag{11}$$

$$\tilde\Omega = \frac{\Omega_\theta}{\Omega_r}\,,\ \tilde V = \frac{V_0}{J\,\Omega_r^2}\,,\ \tilde\alpha = \sqrt{\frac{V_0}{M\,\Omega_r^2}}\,\alpha,\ \tilde R_0 = \sqrt{\frac{M\,\Omega_r^2}{V_0}}\,R_0 \tag{12}$$

$$\tilde\gamma = \frac{\gamma}{V_0}\,,\ \tilde\omega = \frac{\omega}{\Omega_r}\,,\ \tilde\beta = \frac{eE_0}{\sqrt{M\,\Omega_r^2 V_0}}\,. \tag{13}$$

Afterwards we drop the tildes.

The equations of motion are derived from the Hamiltonian (2) and with the use of the expression (9) we obtain

$$\mathrm{i}\,\tau\dot c_n = (E_n^0 + k\,r_n)\,c_n \,-\, \mathrm{i}\gamma\,c_n \,-\, \beta n d_{n\,n-1}\sin(\omega t)\,c_n - (1 - \alpha\,d_{n+1,n})\,c_{n+1} - (1 - \alpha\,d_{n\,n-1})\,c_{n-1} \tag{14}$$

$$\ddot r_n = -r_n - k\,|c_n|^2 \,-\, \frac{R_0}{l_0}\,(1 - \cos\theta_0) \times \Big\{\,\alpha\,\big(\,[c_{n+1}^* c_n + c_{n+1} c_n^*] + [c_n^* c_{n-1} + c_n c_{n-1}^*]\,\big) - \beta n \sin(\omega t)\,|c_n|^2\,\Big\} \tag{15}$$

$$\ddot\theta_{n\,n-1} = -\Omega^2\,\theta_{n\,n-1} \,-\, \frac{R_0^2}{l_0}\,\sin\theta_0\,V \times \Big\{\,\alpha\,[c_n^*\,c_{n-1} \,+\, c_n\,c_{n-1}^*] - \beta n \sin(\omega t)\,|c_n|^2\,\Big\}\,, \tag{16}$$

and the ratio $\tau = \hbar\,\Omega_r/V_0$ determines the time scale separation between the slow electron motion and the fast bond vibrations. We remark that in the limit case of $\alpha = 0$ and constant $E_n^0 = E_0$ the set of coupled equations represents the Holstein system widely used in studies of polaron dynamics in one-dimensional lattices [35]. Furthermore in the linear limit case emerging for $\alpha = k = 0$ and random E_n^0 the Anderson model is obtained [36,37]. (Note that any $E_n^0 c_n$ term on the r.h.s. of equation (14) with constant $E_n^0 = E_0$ can be eliminated by a gauge transformation $c_n \to \exp(-\mathrm{i}E_0 t/\tau)c_n$.)

For a more realistic model of ET in DNA we incorporated the effect of the viscosity of the solvent associated with friction of the electron motion (electronic energy dissipation) which is described by the additional damping term $-\mathrm{i}\gamma c_n$ on the r.h.s. of equation (14).

The values of the scaled parameters are given by $\tau = 0.2589$, $\Omega^2 = [\,0.709 - 1.417\,]\times10^{-2}$, $V = 0.0823$, $R_0 = 34.862$ and $l_0 = 24.590$. In our model study we treat the electron-mode coupling strengths k and α for which no reliable data are available as adjustable parameters. In the subsequent studies we fix the values of these two free parameters such that not too strong deformations of the helix result which is crucial for the harmonic treatment of the dynamics of the structural coordinates. The damping constant lies in the range $\gamma = [0.001, 0.01]$ corresponding to 'life times' on time scales ranging from 10 ps to 100 ps relevant for biological ET.

3 Stationary localized electron-vibron states

In the linear limit case of $\alpha = k = 0$ the (decoupled) isolated electronic tight-binding system $\mathrm{i}\,\dot c_n = E_n^0 c_n - V_{n+1}\,c_{n+1} - V_n\,c_{n-1}$ supports localized solutions (Anderson modes) provided disorder is included in the electronic on-site energy E_n^0 and/or transfer matrix elements V_n [36,37]. On the other hand, for non-vanishing k and/or α the nonlinear interplay between the electronic and the vibrational degrees of freedom leads to the formation of polaronic compounds as localized stationary solutions of the coupled system (14–16) which can be exactly constructed in the absence of the external field and without

the viscous damping term with the help of the nonlinear map approach outlined in [38,39].

We describe briefly the main features of such polaron-like solutions (which we also refer to as standing electron-vibron breathers). The electronic wave function is localized at a lattice site and the envelope of the amplitudes decays monotonically and exponentially with growing distance from this central site (base pair). With either increasing coupling strength(s) k and/or α or growing amount of disorder the degree of electronic localization increases. Hence, we infer that the combined effect of the two localization mechanisms, *viz.*, nonlinear polaron and linear Anderson-mode formation, respectively, leads to enhancement of the degree of localization compared to the case when only one of the two mechanisms acts.

Like the electronic wave function the associated radial and angular displacements are exponentially localized at the central lattice site. Due to the overall non-positive radial and angular amplitudes, the H-bridges get compressed while the helix experiences a local unwinding around the site (base) attributed to the occupation peak of the localized electron.

4 Breather motion initiated by the external periodic field

In this section we study the ET supported by mobile breathers propagating along the DNA. We demonstrate that the coupling of the electron-vibron system, *viz.*, the standing electron-vibron breather, to the periodically varying external field initiates breather motion. Furthermore, despite the electronic energy dissipation (related with the γ term) and energetic disorder, long-lived stable ET can be accomplished.

We consider the two situations of an ordered and disordered DNA model possessing constant and random on-site electronic energies, respectively. The ordered (periodic) case arises, *e.g.*, for synthetically produced DNA molecules consisting of a single type of base pairs (*e.g.*, poly(G)-poly(C) DNA polymers) surrounded by vacuum [40]. On the other hand, for a more general study we take static diagonal disorder in the on-site electronic energy E_n into account. The random values caused, *e.g.*, by the inhomogeneous broadening of the sites of distinct ion pairs with different energies were simulated by random potentials $E_n \in [-\Delta E, \Delta E]$ with mean values $\bar{E} = 0$ and different interval sizes $2\Delta E$. As an illustration of the typical propagation features of the breathers, we represent in Figure 2 the spatio-temporal evolution of the electronic and the two vibrational breather components. We integrated the set of coupled equations (14–16) with a fourth-order Runge-Kutta method and the accuracy of the computation was checked through monitoring the conservation of the norm $\sum_n |c_n(t)|^2 = 1$. The DNA lattice comprises 200 sites and periodic boundary conditions were imposed.

As Figure 2a reveals, under the impact of the external periodic field the (standing) electron breather becomes mobile and propagates directionally along the lattice with a velocity oscillating around a constant mean

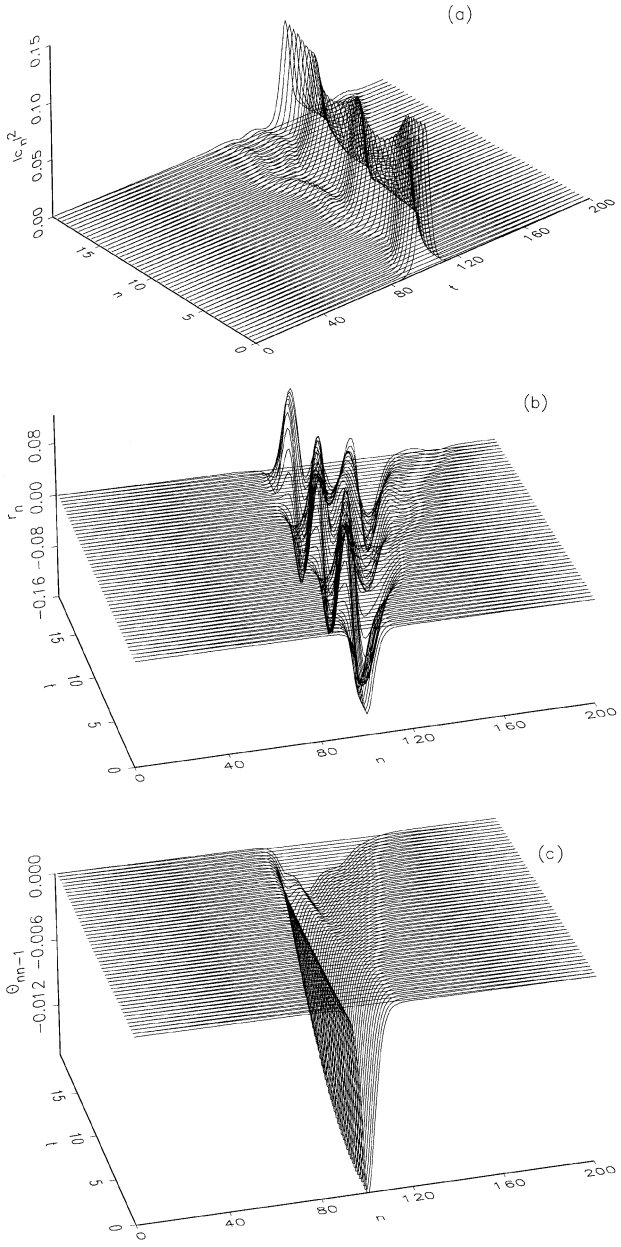

Fig. 2. Breather motion along the DNA in the ordered case. Parameters $\gamma = 0.001$, $\omega = 1$ and $\beta = 0.1$. (a) Electronic breathers. (b) Radial breathers. (c) Angular breathers.

value (see further below). In addition, the amplitude pattern breathes with the frequency of the applied periodic field. At each instant of time, corresponding to a period duration $T = 2\pi/\omega$ of the external field from the moving large-amplitude breather, a small-amplitude breather is radiated which performs oscillatory but confined motions around the lattice position at which it has emerged. The energy content of the main moving breather $E_{el} = \sum_n [\, E_n \, |c_n|^2 - V_{n\,n-1}\, c_n^* c_{n-1} - V_n \, c_n c_{n-1}^* \,]$ gets periodically modulated by the external field and performs oscillations around a constant mean value $\bar{E}_{el}$ in the course of time. There remains some excess energy which can neither be absorbed and carried by the mobile main breather

nor is needed to compensate the energy losses due to friction. This excess energy is deposited into the lattice in the form of additional electronic small-amplitude pinned breathers. Nonetheless, by a suitable choice of the amplitude β of the applied field, the energy balance between the frictional energy loss and the external energy input can be optimized in the sense that there remains (virtually) no excess energy and the 'radiational' creation of the additional small-amplitude breathers is suppressed.

In order to assure that the degree of localization for the moving electron breather is retained, we used the normalized participation number defined as

$$P(t) = \frac{\sum_n |c_n(0)|^4}{\sum_n |c_n(t)|^4} \cdot \tag{17}$$

Since the electronic wave function is normalized, the electron breather is completely confined at a single site if $P = 1$ and is uniformly extended over the lattice if P is of the order N, that is, the number of lattice sites. Hence, P measures how many sites are excited to contribute to the electronic breather pattern. In fact, for the moving breather the participation number stayed close to its initial value throughout the travel of the breather along the DNA lattice.

Similarly, the radial breather component depicted in Figure 2b consists of a moving small-amplitude breather accompanying the electron and additional 'radiationally' generated standing breathers, the amplitudes of which are modulated by the external periodic field. We emphasize that no significant structural deformations of the double helix develop and the maximal amplitude of the stretchings of the hydrogen bonds from the equilibrium length is restricted to values less than 0.04 Å, justifying the harmonic treatment of the corresponding bond potential. In the case of the torsional breather component the radiation effect is not as pronounced as for their electronic and radial counterparts. Nevertheless there appears a moving torsional breather propagating in unison with its electronic and radial counterparts. However, the amplitudes of this moving torsional breather are small compared to the amplitudes of the slowly varying and immobile breather resting at the starting site. Hence, ET in DNA mediated by breathers is connected mainly with radial displacements rather than angular deformations along the transfer path.

For further illustration of the ET we display in Figure 3 the velocity of the electron breather as a function of the field amplitude β and for different values of the driving frequency ω. Interestingly, the dependence of the breather velocity on the field amplitude exhibits a resonance structure and the larger the driving frequency is, the broader is the resonance curve while its peak position shifts towards larger field strengths. Hence, for each frequency of the field there exists an optimal field amplitude providing a maximal possible breather velocity. The value of the latter is higher the lower the frequency of the applied chosen field. In conclusion, with an appropriate choice of the amplitude β of the external field the velocity of the ET can be tuned. We found that coherent ET can be stimulated

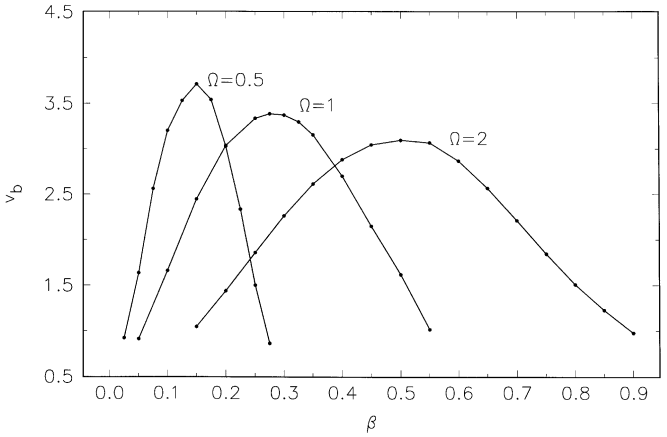

Fig. 3. The velocity of the moving electron breather as a function of the amplitude of the external periodic field β for different frequencies as indicated on the graphs.

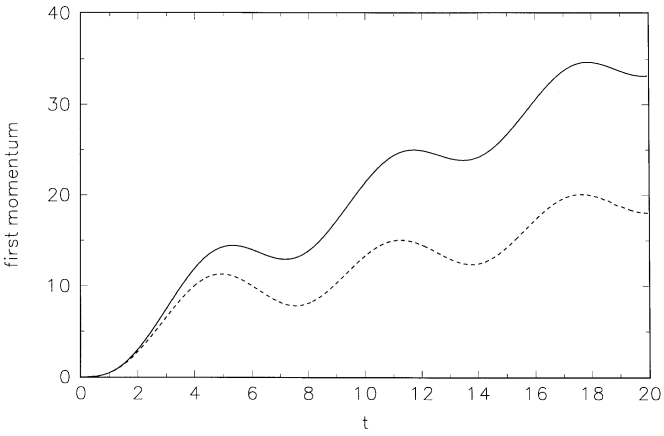

Fig. 4. Time-evolution of the first momentum of the electronic amplitude. Parameters: $\gamma = 0.001$, $\omega = 1$ and $\beta = 0.1$. Full line: ordered case of constant on-site energy $E_n = E_0 = 0$; dashed line: random on-site energies with width $\Delta E = 0.1$ and mean value $\bar{E} = 0$.

when the frequency of the applied field lies in the range $0.1 \lesssim \omega \lesssim 3.25$.

Figure 4 shows the time evolution of the first momentum of the electronic amplitude distribution $\bar{n}(t) = \sum_n n\,|c_n(t)|^2$, indicating the mobility of the breather in the ordered (full line) as well as a disordered case (dashed line), respectively. One concludes that the breather moves effectively unidirectionally along the lattice although its center performs oscillations around a straight line the slope of which (in the depicted time versus position plane) determines the breather velocity. Concerning the activation of breather motion we observe that the immediate initial energy injection through the external field supplies kinetic energy and the breather starts to move in a direction dictated by the initial phase of the external field. This instantaneous energy deposition proceeds similarly to the kick mechanism (relying on the so called pinning mode) used to initiate breather motions in discrete lattice system [41]. However, in the case of the kick mechanism the

energy transfer is limited to an instant of time whereas for the driving with the external periodic field energy is permanently delivered, which is also needed to compensate the incessant energetic losses due to friction. Moreover, for the kick mechanism the pinning mode (as a localized mode of the corresponding tangent system with certain spatial shape) has to be designed before its application as an appropriate perturbation of the velocity component of the breather. In the current case of external driving no special pattern of the imposed external field is requested, which can rather be of a general periodic type. The temporal periodic modulation of the breather velocity proceeds in resonance with the periodic external force. When the amplitude of the external field grows (diminishes) during the time intervals $(4n+3)\pi/(2\omega) \leq t < (4n+5)\pi/(2\omega)$, $((4n+1)\pi/(2\omega) \leq t < (4n+3)\pi/2(\omega))$ with $n = 0, 1, 2, ..$, the breather motion is accelerated (retarded) and hence, the velocity exceeds (falls short of) its mean value.

As the influence of disorder is concerned, we find that the stronger the degree of disorder is, the slower propagates the corresponding breather. We underline that the linear Anderson modes are generally immobile [36,37], whereas the nonlinear breathers may be mobile [42]. In our case the standing localized states of the disordered and nonlinear DNA lattice system represent combinations of linear Anderson modes and nonlinear breathers and their respective contribution to a localized state depend on the relative ratio of the amount of diagonal disorder ΔE and the nonlinear interaction strength measured by the value(s) of k and/or α.

Equivalently, starting with the ordered case, *i.e.*, $\Delta E = 0$, the corresponding localized state originates exclusively from the nonlinear interaction between the electronic subsystem and the vibrational ones and the width of the associated amplitude patterns, *i.e.*, the degree of localization, is governed by the strength of the nonlinear interaction. When additionally disorder is taken into account, the degree of localization increases compared to the purely nonlinear case which diminishes also the ability to move the localized state due to its stronger pinning to the discrete lattice.

However, for undercritical amount of disorder, ΔE, the localized states maintain to such an sufficient extent their nonlinear breather character that the initiation of its motion is possible and thus conductivity persists. This behavior is illustrated in Figure 5 showing the breather velocity as a function of the external field amplitude β for a frequency $\omega = 1$ and for growing amount of disorder, ΔE. With increasing ΔE the maximal possible breather velocity becomes smaller and mobility is achievable up to a moderate strength of disorder $\Delta E \lesssim 0.25$. It was indeed experimentally found that the random sequence of λ-DNA is an electrical conductor [9].

Finally, for overcritical amount of disorder $\Delta E \gtrsim 0.25$ the initiation of coherent long-range ET along the DNA lattice is suppressed. The motion of the localized state (dominantly of linear Anderson-mode type rather than a nonlinear breather) is restricted to oscillatory motions around its starting position which is in compliance with

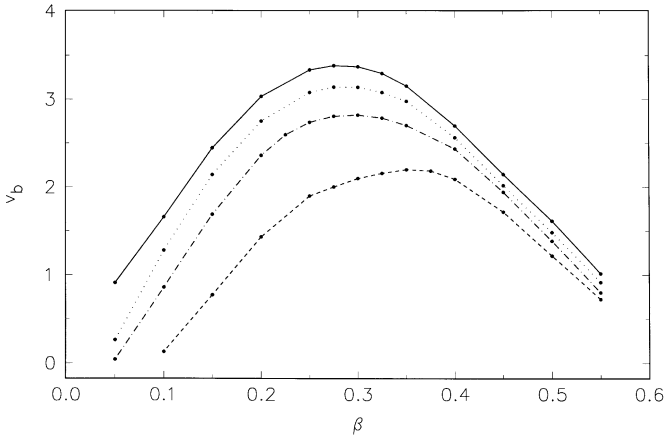

Fig. 5. Dependence of the velocity of the electron breather on the field amplitude β and for different degree of randomness in the on-site energies. Assignment of the line types to the increasing amount of disorder: Full line ($\Delta E = 0$), dotted line ($\Delta E = 0.025$), dashed dotted line ($\Delta E = 0.05$) and dashed line ($\Delta E = 0.1$).

the fact that the linear Anderson-modes are actually immobile. The amplitudes of these oscillations, *viz.*, the excursions form the starting site, diminish with more enlarged ΔE going along with gradual enhancement of the pinning of the breather.

In reference [22] polaronic charge transport in DNA was studied in the frame of an one-dimensional lattice model for which the charge carrying unit is coupled semiclassically to a nonlinear lattice model describing the large-amplitude fluctuations of the base pairs. It was demonstrated that when the charge carrier part of a (static) polaron without its associated lattice deformations is placed initially in a randomly fluctuating chain appropriate base pair distortions are induced which causes the motion of the carrier in a random direction. When the dynamically random deformations of the hydrogen bonds exceed a certain critical size, the polaron interacts strongly with them, and polaron trapping is observed.

We demonstrate now that the application of a low-frequency external field offers a possibility to control the range of ET in DNA. Our results are summarized in Figure 6 depicting the temporal behavior of the first momentum of the electronic occupation probability for relatively strong disorder $\Delta E = 0.2$. The frequency of the imposed external field is $\omega = 0.1$ and its amplitude β is varied. For $\beta = 0.2$ we find that in an initial phase the center of the electron breather propagates steadily away from its starting position and moves over more than thirty sites, corresponding to directional long-range ET. Then the direction of the motion is reversed but the electron breather does not return completely to its starting position. Eventually, the electron breather oscillates around a fixed lattice site (base) being 22 sites apart from the starting position. Remarkably, when the amplitude β is enlarged, the maximum of these oscillations diminishes while the frequency increases. Furthermore, the central position around which the oscillations take place is shifted downwards to lower

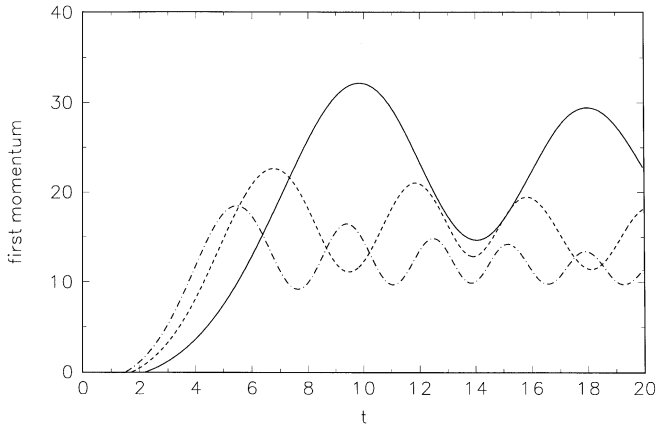

Fig. 6. The temporal behavior of the position of the electron breather center in the presence of a low frequency external field. Parameters $\omega = 0.1$ and diagonal disorder $\Delta E = 0.1$. Full line ($\beta = 0.2$), dashed line ($\beta = 0.4$) and dashed dotted line ($\beta = 0.6$).

lattice sites. Hence, with the choice of an appropriate amplitude of the low-frequency external field, the control of the range of the electron excursion along the DNA is possible.

The results of our numerical simulations suggest that in order to activate and control the ET in DNA, strong electrical fields with field strengths of the order of $10^6 - 10^7$ V/cm and oscillations which are fast compared to the electronic transfer process are needed. In references [28–31] the proposed control of longe-rang ET in molecular systems utilizing a strong periodic field is based on similar assumptions with respect to the field strengths and the time scale separation between the fast oscillations of the external field and the electron transfer rate.

5 Summary

In the present work we have studied the ET mechanism in an idealized DNA model relying on the coupling of the charge to vibrational modes of DNA. For the purpose of nonlinear dynamical studies of DNA, strong simplification is needed concerning the structure of the molecule. As one restriction, in our model no inner degrees of freedom of the bases have been considered. This seems justified as the small and fast vibrational motions of the individual atoms are separated from the larger and slower motions of the atom groups by a different time scale. Further, we have not distinguished between the four different base types and have treated each base as a single entity of fixed mass. Finally, the coupling of the electronic amplitude to ambient solvent coordinates has been conveniently modeled by a simple friction term inducing electronic energy dissipation. Particularly, for a more elaborate study of ET through DNA the accompaniment of the ET process by electronic energy dissipation resulting from the effects of a variety of both internal and external influences have to be considered in more detail. Furthermore, real DNA molecules exhibit random structural imperfections of their double helix caused, *e.g.*, by the random base sequence and the deforming impact of the chemical surroundings. In addition, the varying hydrophobic potential of the base pair interactions depending on the ambient aqueous solvent may leave the helix structures in irregularly distorted shapes. Accordingly, for an improvement of our model, solvent effects can be included by taking into account real geometries of DNA obtained experimentally.

Within in the frame of our simple DNA model for the λ-form of DNA, the double helix structure has been modeled by a three-dimensional oscillator network and within the base-pair picture angular twist motions of the base pairs as well as their radial vibrations have been taken into account. The nonlinear interaction between the electronic and the vibrational subsystems is responsible for the formation of standing electron-vibron breathers which have been constructed with the help of a nonlinear map approach. In our investigations of ET in our DNA model we have focused interest on the initiation of long-range and stable breather motion along the DNA structure, including also energetic disorder inherent to any real DNA molecule. Furthermore, the effects of viscosity of the water structure around DNA leading to electronic energy dissipation have been incorporated in a damping term. We have demonstrated that an applied electric field activates the long-range coherent motion of breathers consisting of traveling electron, radial and twist components along the bases of the DNA strands. Moreover, varying the amplitude of the applied field one is able to tune the propagation velocity of the breather which can be exploited to control ET in DNA. Regarding the role of energetic disorder, we have found that the mobile breathers sustain moderate amount of randomness, and conductivity persists. However, for overcritical strength of disorder the breather motion is inhibited preventing conductivity. Finally, with the application of a low-frequency external field the breather can be steered to a desired lattice position through amplitude-tuning of the applied field, where the chosen initial phase of the latter governs the propagation direction. In this way targeted control of the ET in DNA is achievable. We hope that our proposed theoretical mechanism for the control of ET in DNA stimulates experimental work in this direction. These experiments could involve direct measurement of the electrical current (I-V-characteristics) as a function of the external electrical potential applied across the DNA molecule (for details see *e.g.* [9]). Alternatively, the DNA conductivity can be quantitatively assessed from the length dependence of the electron transfer rates as a function of the external field strength (see *e.g.* [7,8]). Especially the last method offers the possibility to monitor the steered electron path.

The author acknowledges support by the Deutsche Forschungsgemeinschaft *via* a Heisenberg fellowship (He 3049/1-1).

References

1. M.D. Purugganan *et al.*, Science **247**, 6548 (1988); D.N. Beratan *et al.*, *ibid.* **258**, 1740 (1997); C.J. Murphy *et al.*, *ibid.* **262**, 1025 (1993); M.R. Arkin *et al.*, *ibid.* **273**, 475 (1996); P.J. Dandliker, R.E. Holmlin, J.K. Barton, *ibid.* **257**, 1465 (1997)
2. D.D. Eley, D.I. Spivey, Trans. Faraday Soc. **58**, 411 (1962)
3. D.B. Hall, R.E. Holmkin, J.K. Barton, Nature **382**, 731 (1996)
4. D.B. Hall, J.K. Barton, J. Am. Chem. Soc. **119**, 5045 (1997)
5. M.R. Arkin, E.D.A. Stemp, S.C. Pulver, J.K. Barton, Chem. Biol. **4**, 369 (1997)
6. Y. Okahata, T. Kobayashi, K. Tanaka, M. Shimomura, J. Am. Chem. Soc. **120**, 6165 (1998)
7. F.D. Lewis *et al.*, Science **277**, 673 (1997)
8. E. Meggers, M.E. Michel-Beyerle, B. Giese, J. Am. Chem. Soc. **120**, 12950 (1998)
9. H.-W. Fink, C. Schönenberger, Nature **398**, 407 (1999)
10. P. Tran, B. Alavi, G. Gruner, Phys. Rev. Lett. **85**, 1564 (2000)
11. B. Giese, J. Amaudrut, A.-K. Köhler, M. Spormann, S. Wessely, Nature **412**, 318 (2001)
12. M. Ratner, Nature **397**, 480 (1999)
13. A.Yu. Kasumov, M. Kociak, S. Gueron, B. Reulet, V.T. Volkov, D.V. Klinov, H. Bouchiat, Science **291**, 280 (2001)
14. E. Braun, Y. Eichen, U. Sivan, G. Ben-Yoseph, Nature **391**, 775 (1998)
15. D. Ly *et al.*, J. Am. Chem. Soc. **118**, 8747 (1996)
16. J. Jortner, Proc. Nat. Acad. Sci. USA, **95**, 12759 (1998)
17. R. Bruinsma, G. Grüner, M.R. D'Orsogna, J. Rudnick, Phys. Rev. Lett. **85**, 4393 (2000)
18. Z.G. Yu Xueyu Song, Phys. Rev. Lett. **86**, 6018 (2001)
19. Z. Hermon, S. Caspi, E. Ben-Jacob, Europhys. Lett. **43**, 482 (1998)
20. E. Conwell, S.V. Rakhmanova, Proc. Nat. Acad. Sci. USA, **97**, 4556 (2000); S.V. Rakhmanova, E.M. Conwell, J. Phys. Chem. B **105**, 2056 (2001)
21. D. Ly, L. Sanii, G.B. Schuster, J. Am. Chem. Soc. **121**, 9400 (1999)
22. S. Komineas, G. Kalosakas, A.R. Bishop, Phys. Rev. E **65**, 061905 (2002)
23. D.M. Basko, E.M. Conwell, Phys. Rev. E **65**, 061902 (2002)
24. M. Peyrard, A.R. Bishop, Phys. Rev. Lett. **62**, 2755 (1989)
25. L.V. Yakushevich, Quart. Rev. Biophys. **26**, 201 (1993)
26. M. Barbi, S. Cocco, M. Peyrard, Phys. Lett. A **253**, 358 (1999)
27. M. Morillo, R.I. Cukier, J. Chem. Phys. **98**, 4548 (1993)
28. Y. Dakhnovskii, J. Chem. Phys. **100**, 6492 (1994)
29. Y. Dakhnovskii, D.G. Evans, H.J. Kim, R.D Coalson, J. Chem. Phys. **103**, 5459 (1995)
30. I.A. Goychuk, E.G. Petrov, V. May, Chem. Phys. Lett. **253**, 428 (1996)
31. I.A. Goychuk, E.G. Petrov, V. May, J. Chem. Phys. **106**, 4522 (1997).
32. L. Stryer, *Biochemistry* (Freeman, New York, 1995)
33. Y.-J. Ye, R.-S. Chen, A. Martinez, P. Otto, J. Ladik, Sol. Stat. Comm. **112**, 139 (1999)
34. S. Cocco, R. Monasson, J. Chem. Phys. **112**, 10017 (2000)
35. T.D. Holstein, Ann. Phys. NY **8**, 325, 343 (1959)
36. P.W. Anderson, Phys. Rev. **109**, 1492 (1958)
37. N.F. Mott, Adv. Phys. **10**, 107 (1961)
38. G. Kalosakas, S. Aubry, G.P. Tsironis, Phys. Rev. B **58**, 3094 (1998)
39. N.K. Voulgarakis, G.P. Tsironis, Phys. Rev. B **63**, 14302 (2001)
40. D. Porath, A. Bezryadin, S. de Vries, C. Dekker, Nature **403**, 635 (2000)
41. D. Chen, S. Aubry, G.P. Tsironis, Phys. Rev. Lett. **77**, 4776 (1996)
42. S. Flach, C.R. Willis, Phys. Rep. **295**, 181 (1998)